Technical note: on LA–ICP-MS U–Pb dating of unetched and etched apatites

Fanis Abdullin[1], Luigi A. Solari[2], Jesús Solé[3], Carlos Ortega-Obregón[2]

[1]CONACyT–Centro de Geociencias, Campus Juriquilla, UNAM, Querétaro, 76230, Mexico

[2]Centro de Geociencias, Campus Juriquilla, UNAM, Querétaro, 76230, Mexico

[3]LANGEM, Instituto de Geología, UNAM, Ciudad Universitaria, CDMX, 04510, Mexico

Correspondence: Fanis Abdullin (fanis@geociencias.unam.mx)

Abstract

The same unetched and chemically etched apatite crystals from five rock samples were dated by U–Pb method via laser ablation inductively-coupled plasma mass spectrometry (LA–ICP-MS). The objective of this study is to test whether chemical etching required for apatite fission track analysis impacts the precision and accuracy of apatite U–Pb geochronology. The results of this experiment suggest that etching has insignificant effects on the accuracy of apatite U–Pb ages obtained by LA–ICP-MS. Therefore, LA–ICP-MS is reliable for U–Pb analysis as part of apatite fission track and U–Pb double dating.

Short summary

Unetched and etched apatite grains from five samples were dated by U–Pb method using laser ablation inductively-coupled plasma mass spectrometry. Our experiment indicates that etching needed for apatite fission track dating has insignificant effects on obtaining accurate U–Pb ages;

thus, the laser ablation-based technique may be used for apatite fission track and U–Pb double dating.

1 Introduction

Apatite, $Ca_5(PO_4)_3[F,Cl,OH]$, is the most common phosphate mineral in the Earth's crust and can be found in practically all igneous and metamorphic rocks, in many ancient and recent sediments as well as in certain mineral deposits (Piccoli and Candela, 2002; Morton and Yaxley, 2007; Webster and Piccoli, 2015). This accessory mineral is often used as a natural thermochronometer for fission track, helium, U–Th and U–Pb dating (e.g., Zeitler et al., 1987; Wolf et al., 1996; Ehlers and Farley, 2003; Hasebe et al., 2004; Donelick et al., 2005; Chew and Donelick, 2012; Chew et al., 2014; Cochrane et al., 2014; Liu et al., 2014; Spikings et al., 2015; Glorie et al., 2017). Presently, apatite fission track (AFT) ages can be obtained rapidly by using laser ablation inductively-coupled plasma mass spectrometry (LA–ICP-MS) for direct measurement of "parent nuclides", i.e., ^{238}U contents (Cox et al., 2000; Svojtka and Košler, 2002; Hasebe et al., 2004, 2009; Donelick et al., 2005; Abdullin et al., 2014, 2016, 2018; Vermeesch, 2017). The LA–ICP-MS technique may be used to measure ^{238}U for AFT dating, together with Pb isotopes needed for U–Pb dating (e.g., Chew and Donelick, 2012; Liu et al., 2014; Glorie et al., 2017; Bonilla et al., 2020; Nieto-Samaniego et al., 2020).

Hasebe et al. (2009) previously performed an important experimental study, during which they demonstrated that chemical etching required for apatite/zircon fission track dating does not interfere with U analysis by LA–ICP-MS. After chemical etching of apatite, a smaller volume of ablated material is analyzed by LA–ICP-MS. The influence of etching needed for AFT dating on the precision and accuracy of dating the same crystals by U–Pb using LA–ICP-MS remains to be quantified. To investigate this issue, the same unetched and etched apatite grains extracted from five rock samples were analyzed via LA–ICP-MS for U–Pb dating. The chosen rock samples have either emplacement or metamorphic ages ranging from the Cretaceous to the Neoproterozoic (see Table 1 for further details).

--- Table 1 ---

2 Sample descriptions

2.1 OV-0421 (Tres Sabanas Pluton, Guatemala)

This sample is a two mica-bearing deformed granite belonging to the Tres Sabanas Pluton, which is located northwest of Guatemala City, Guatemala. For sample OV-0421, an emplacement age of 115 ± 4 (2σ) Ma was proposed based on zircon U–Pb data (Torres de León, 2016). A cooling age of 102 ± 1 (2σ) Ma, obtained with K–Ar (on biotite), was also reported by the same author.

2.2. MCH-38 (Chiapas Massif Complex, Mexico)

MCH-38 is an orthogneiss from the Permian Chiapas Massif Complex. This rock was sampled to the west of Unión Agrarista, the State of Chiapas, southeastern Mexico. There is no reported age for this sample. Some zircon U–Pb dates obtained for the Chiapas Massif Complex (Weber et al., 2007, 2008; Ortega-Obregón et al., 2019) suggest that a Lopingian (260–252 Ma) crystallization or metamorphic age may be assumed for sample MCH-38.

2.3 TO-AM (Totoltepec Pluton, Mexico)

TO-AM is a granitic rock, sampled ca. 5 km west of Totoltepec de Guerrero, the State of Puebla, southern Mexico. There is no reported radiometric data for sample TO-AM. Previous geological studies indicate that the Pennsylvanian–Cisuralian Totoltepec Pluton was emplaced over a ca. 23 million year period (from ca. 308 to ca. 285 Ma; e.g., Kirsch et al., 2013).

2.4 CH-0403 (Altos Cuchumatanes, Guatemala)

CH-0403 was collected 5 km ESE of Barillas, in the Altos Cuchumatanes, Guatemala. It consists of a gray to green granodiorite. Five zircon aliquots of sample CH-0403 were dated using isotope dilution thermal-ionization mass spectrometry, yielding a lower intercept date of 391 ± 8 (2σ) Ma that is interpreted as its approximate crystallization age (Solari et al., 2009).

2.5 OC-1008 (Oaxacan Complex, Mexico)

This sample is a paragneiss from the Grenvillian Oaxacan Complex, southern Mexico. OC-1008 was collected in the federal road which connects Nochixtlán to Oaxaca. It was demonstrated that this sample underwent granulite facies metamorphism at 1000–980 Ma (Solari et al., 2014).

3 Analytical procedures

Accessory minerals were concentrated using conventional mineral separation techniques such as rock crushing, sieving, Wilfley table, Frantz magnetic separator, and bromoform. Approximately 300 apatite grains were extracted from each rock sample and mounted with their surfaces parallel to the crystallographic *c*-axis in a 2.5 cm diameter epoxy mount. Mounted crystals were polished to expose their internal surfaces (i.e., up to 4π geometry). For this experiment, complete crystals lacking visible inclusions and other defects, such as cracks, were carefully selected for analysis. Sample preparation was performed at Taller de Molienda and Taller de Laminación, Centro de Geociencias (CGEO), Campus Juriquilla, Universidad Nacional Autónoma de Mexico (UNAM).

Single spot analyses were performed with a Resonetics RESOlution™ LPX Pro (193 nm, ArF excimer) laser ablation system, coupled to a Thermo Scientific iCAP™ Qc quadrupole ICP-MS at Laboratorio de Estudios Isotópicos (LEI), CGEO, UNAM. During this experimental work, LA–ICP-MS-based sampling was performed in central parts of the selected apatite grains before and after chemical etching (in 5.5M HNO_3 at 21 °C for 20 s to reveal spontaneous fission tracks), as shown schematically in Fig. 1. The LA–ICP-MS protocol used for apatite analyses, as given in Table 2, was established on the basis of numerous experiments carried out at LEI during the past five years, and can be used for U–Pb and fission track double dating plus multielemental analysis (Abdullin et al., 2018; Ortega-Obregón et al., 2019). Corrected isotopic ratios and errors were calculated using Iolite 3.5 (Paton et al., 2011) and the VizualAge data reduction scheme (Petrus and Kamber, 2012). UcomPbine (Chew et al., 2014) was used to model $^{207}Pb/^{206}Pb$ initial values and thus force a ^{207}Pb correction that considers the common Pb (non-radiogenic Pb) incorporated by apatite standards at the moment of their crystallization (see also Ortega-Obregón et al., 2019). The "First Mine Discovery" apatite from Madagascar, with a mean U–Pb age of ca. 480 Ma (Thomson et al., 2012; Chew et al., 2014), was used as a primary reference material. The results for measured isotopes using NIST-612 (Pearce et al., 1997) were normalized using ^{43}Ca as an internal standard and taking an average CaO content of 55%.

Tera–Wasserburg Concordia diagrams (T–W; Tera and Wasserburg, 1972) are used in apatite U–Pb dating, because the LA–ICP-MS-derived U–Pb results are generally discordant. The lower intercept in the T–W plot is considered as a mean apatite U–Pb age that should have geological significance (crystallization or cooling age, the age of mineralization or metamorphic event). Apatite U–Pb ages were calculated with IsoplotR (Vermeesch, 2017, 2018) and described below. Detailed information on U–Pb experiments is given in Table S1 in the Supplement.

--- Figure 1 ---

--- Table 2 ---

4 Results

4.1 OV-0421

For rock sample OV-0421, 41 unetched apatites yielded a lower intercept age of 106 ± 4 (2σ) Ma with a mean square weighted deviation (MSWD) of 1.07, passing the chi-squared test with the $P(\chi^2)$ value of 0.35 (see in Fig. 2). Practically the same U–Pb date, 107 ± 5 (2σ) Ma, was obtained after chemical etching of the same apatite grains, yielding a MSWD of 1.13 and a $P(\chi^2)$ of 0.27. Both these apatite U–Pb ages lie between the zircon U–Pb date of 115 ± 4 (2σ) Ma (i.e., crystallization age) and the biotite K–Ar age of 102 ± 1 (2σ) Ma (i.e., cooling age), which were previously obtained for the same granite sample by Torres de León (2016).

4.2. MCH-38

For orthogneiss sample MCH-38, the lower intercept in T–W yielded a U–Pb age of 245 ± 6 (2σ) Ma (obtained from 41 unetched apatites) with a MSWD of 0.28 and a $P(\chi^2)$ of 1. Etched apatite grains from MCH-38 yielded an age of 240 ± 4 (2σ) Ma with a MSWD of 0.36 and a $P(\chi^2)$ of 1 (Fig. 2). Our U–Pb results are in close agreement with geochronological data reported from the Chiapas Massif Complex in previous studies (Damon et al., 1981; Torres et al., 1999; Schaaf et al., 2002; Ortega-Obregón et al., 2019). For instance, Torres et al. (1999) compiled biotite K–Ar ages, most of which lie within Early–Middle Triassic period. Triassic cooling ages in the Chiapas Massif Complex were also detected by Rb–Sr in mica–whole rock pairs that range from 244 ± 12 (2σ) Ma to 214 ± 11 (2σ) Ma (Schaaf et al., 2002).

4.3 TO-AM

Unetched apatites (32 crystals; Fig. 2) from granite TO-AM yielded a lower intercept date of 303 ± 5 (2σ) Ma with a MSWD of 0.6 and a $P(\chi^2)$ of 0.96. After etching, a slightly younger age of 299 ± 3 (2σ) Ma was obtained, with a MSWD of 0.89 and a $P(\chi^2)$ of 0.65. These apatite U–Pb ages are in line with the zircon U–Pb ages of 306 ± 2 (2σ) Ma to 287 ± 2 (2σ) Ma reported for the Pennsylvanian–Cisuralian Totoltepec Pluton (e.g., see details in Kirsch et al., 2013).

4.4 CH-0403

36 unetched apatite grains from sample CH-0403 yielded a lower intercept U–Pb age of 345 ± 10 (2σ) Ma with a MSWD of 0.7 and a $P(\chi^2)$ of 0.9, whereas etched grains yielded an age of 334 ± 8 (2σ) Ma with a MSWD of 1.37 and a $P(\chi^2)$ of 0.08 (Fig. 2). These cooling dates are considerably younger if compared to the CH-0403 emplacement age of 391 ± 8 (2σ) Ma (Solari et al., 2009).

4.5 OC-1008

41 unetched apatites belonging to sample OC-1008 yielded a U–Pb age of 839 ± 12 (2σ) Ma with a MSWD of 0.98 and a $P(\chi^2)$ of 0.50. After etching, the same apatite crystals yielded an age of 830 ± 10 (2σ) Ma with a MSWD of 1.24 and a $P(\chi^2)$ of 0.14 (Fig. 2). Both these apatite U–Pb ages are significantly younger than the age of granulite facies metamorphism in the Grenville-aged Oaxacan Complex (1 Ga to 980 Ma, Solari et al., 2014), and thus, should be considered as cooling ages.

--- Figure 2 ---

5 Discussion and concluding remarks

Most rock samples, except OV-0421, yielded slightly younger apatite U–Pb ages after chemical etching (up to 3.3% in sample CH-0403). However, the lower intercept U–Pb ages obtained from unetched apatite grains are indistinguishable within error from the U–Pb ages obtained on the same etched grains (see diagram in Fig. 3). The results of this experiment demonstrate that chemical etching required for AFT analysis has negligible effects on the accuracy of apatite U–Pb ages determined via LA–ICP-MS. Thus, as a main conclusion of this study, LA–ICP-MS can be used for simultaneous AFT and U–Pb ages double dating, as it was already done in some previous studies (e.g., Chew and Donelick, 2012; Liu et al., 2014; Glorie et al., 2017; Bonilla et al., 2020; Nieto-Samaniego et al., 2020).

--- Figure 3 ---

Supplement

The supplement related to this article is available online at: https://...

Author contributions

Conceptualisation, investigation, and writing of the original draft were done by FA. LS and COO provided technical support. LS and JS acquired funding and resources, supervised the study, and reviewed the manuscript.

Competing interests

The authors declare that they have no conflict of interest.

Acknowledgements

The authors are grateful to Juan Tomás Vázquez Ramírez and Ofelia Pérez Arvizu for their help with sample preparation for this study. Professor Stuart Thomson is acknowledged for sharing Madagascar apatite. Dr. Michelangelo Martini kindly provided sample TO-AM that was useful for our experimental study. Dr. Ziva Shulaker, Dr. Jakub Sliwinski, and Professor Axel Schmitt are acknowledged for their constructive comments that improved our manuscript significantly.

Financial support

This research has been supported by PAPIIT DGAPA UNAM (grant no. IN101520 to LS).

Figure caption

Figure 1

Illustration displaying the LA–ICP-MS-based U–Pb dating of the same apatite crystal before and after chemical etching (i.e., etched in 5.5M nitric acid at 21 °C for 20 s). Spot diameter of 60 µm.

Figure 2

Tera–Wasserburg Concordia diagrams for the U–Pb results of unetched and etched apatites from samples OV-0421, MCH-38, TO-AM, CH-0403, and OC-1008. MSWD – mean square weighted deviation, Ngr – number of grains dated. Errors are given in 2σ.

Figure 3

Plot showing the lower intercept U–Pb ages obtained on unetched and etched apatite grains.

References

Abdullin, F., Solé, J., and Solari, L.: Datación mediante trazas de fisión y análisis multielemental con LA-ICP-MS del fluorapatito de Cerro de Mercado (Durango, México), Revista Mexicana de Ciencias Geológicas, 31, 395–406, 2014.

Abdullin, F., Solé, J., Meneses-Rocha, J.D.J., Solari, L., Shchepetilnikova, V., and Ortega-Obregón, C.: LA-ICP-MS-based apatite fission track dating of the Todos Santos Formation sandstones from the Sierra de Chiapas (SE Mexico) and its tectonic significance, International Geology Review, 58, 32–48, 2016, https://doi.org/10.1080/00206814.2015.1055596.

Abdullin, F., Solari, L., Ortega-Obregón, C., and Solé, J.: New fission-track results from the northern Chiapas Massif area, SE Mexico: trying to reconstruct its complex thermo-tectonic history, Revista Mexicana de Ciencias Geológicas, 35, 79–92, https://doi.org/10.22201/cgeo.20072902e.2018.1.523, 2018.

Bonilla, A., Franco, J. A., Cramer, T., Poujol, M., Cogné, N., Nachtergaele, S., and De Grave, J.: Apatite LA-ICP-MS U–Pb and fission-track geochronology of the Caño Viejita gabbro in E-Colombia: Evidence for Grenvillian intraplate rifting and Jurassic exhumation in the NW Amazonian Craton, Journal of South American Earth Sciences, 98, 102438, https://doi.org/10.1016/j.jsames.2019.102438, 2020.

Chew, D. M., and Donelick, R. A.: Combined apatite fission track and U-Pb dating by LA-ICP-MS and its application in apatite provenance analysis, Quantitative Mineralogy and Microanalysis of Sediments and Sedimentary Rocks: Mineralogical Association of Canada, Short Course, 42, 219–247, 2012.

Chew, D. M., Petrus, J. A., and Kamber, B. S.: U–Pb LA–ICPMS dating using accessory mineral standards with variable common Pb, Chemical Geology, 363, 185–199, https://doi.org/10.1016/j.chemgeo.2013.11.006, 2014.

Cochrane, R., Spikings, R. A., Chew, D., Wotzlaw, J. F., Chiaradia, M., Tyrrell, S., Schaltegger, U., and Van der Lelij, R.: High temperature (> 350 °C) thermochronology and mechanisms of Pb loss in apatite, Geochimica et Cosmochimica Acta, 127, 39–56, https://doi.org/10.1016/j.gca.2013.11.028, 2014.

Cox, R., Košler, J., Sylvester, P., and Hodych, P.: Apatite fission-track (FT) dating by LAM-ICP-MS analysis, Goldschmidt Conference, Oxford, UK, Journal of Conference Abstracts, 5, p. 322, 2000.

Damon, P. E., Shafiqullah, M., and Clark, K. F.: Age trends of igneous activity in relation to metallogenesis in the southern Cordillera, Tucson, Arizona, Arizona Geological Society Digest, 14, 137–153, 1981.

Donelick, R. A., O'Sullivan, P. B., and Ketcham, R. A.: Apatite fission-track analysis, Reviews in Mineralogy and Geochemistry, 58, 49–94, https://doi.org/10.2138/rmg.2005.58.3, 2005.

Ehlers, T. A., and Farley, K. A.: Apatite (U–Th)/He thermochronometry: methods and applications to problems in tectonic and surface processes, Earth and Planetary Science Letters, 206, 1–14, https://doi.org/10.1016/S0012-821X(02)01069-5, 2003.

Glorie, S., Alexandrov, I., Nixon, A., Jepson, G., Gillespie, J., and Jahn, B. M.: Thermal and exhumation history of Sakhalin Island (Russia) constrained by apatite U-Pb and fission track thermochronology, Journal of Asian Earth Sciences, 143, 326–342, https://doi.org/10.1016/j.jseaes.2017.05.011, 2017.

Hasebe, N., Barbarand, J., Jarvis, K., Carter, A., and Hurford, A. J.: Apatite fission-track chronometry using laser ablation ICP-MS, Chemical Geology, 207, 135–145, https://doi.org/10.1016/j.chemgeo.2004.01.007, 2004.

Hasebe, N., Carter, A., Hurford, A. J., and Arai, S.: The effect of chemical etching on LA–ICP-MS analysis in determining uranium concentration for fission-track chronometry, Geological Society, London, Special Publications, 324, 37–46, https://doi.org/10.1144/SP324.3, 2009.

Kirsch, M., Keppie, J. D., Murphy, J. B., and Lee, J. K.: Arc plutonism in a transtensional regime: the late Palaeozoic Totoltepec pluton, Acatlán Complex, southern Mexico, International Geology Review, 55, 263–286, https://doi.org/10.1080/00206814.2012.693247, 2013.

Liu, W., Zhang, J., Sun, T., Wang, J.: Application of apatite U–Pb and fission-track double dating to determine the preservation potential of magnetite–apatite deposits in the Luzong and Ningwu volcanic basins, eastern China, Journal of Geochemical Exploration, 138, 22–32, https://doi.org/10.1016/j.gexplo.2013.12.006, 2014.

Morton, A., and Yaxley, G.: Detrital apatite geochemistry and its application in provenance studies, Special Papers, Geological Society of America, 420, 319, https://doi.org/10.1130/2006.2420(19), 2007.

Nieto-Samaniego, A. F., Olmos-Moya, M. D. J. P., Levresse, G., Alaniz-Alvarez, S. A., Abdullin, F., del Pilar-Martínez, A., and Xu, S.: Thermochronology and exhumation rates of granitic intrusions at Mesa Central, Mexico, International Geology Review, 62, 311–319, https://doi.org/10.1080/00206814.2019.1602789, 2020.

Ortega-Obregón, C., Abdullin, F., Solari, L., Schaaf, P., and Solís-Pichardo, G.: Apatite U-Pb dating at UNAM laboratories: analytical protocols and examples of its application, Revista Mexicana de Ciencias Geológicas, 36, 27–37, https://doi.org/10.22201/cgeo.20072902e.2019.1.749, 2019.

Paton, C., Hellstrom, J., Paul, B., Woodhead, J., Hergt, J.: Iolite: Freeware for the visualisation and processing of mass spectrometric data, Journal of Analytical Atomic Spectrometry, 26, 2508–2518, https://doi.org/10.1039/C1JA10172B, 2011.

Pearce, N. J., Perkins, W. T., Westgate, J. A., Gorton, M. P., Jackson, S. E., Neal, C. R., and Chenery, S. P.: A compilation of new and published major and trace element data for NIST SRM 610 and NIST SRM 612 glass reference materials, Geostandards newsletter, 21, 115–144, https://doi.org/10.1111/j.1751-908X.1997.tb00538.x, 1997.

Petrus, J. A., and Kamber, B. S.: VizualAge: A novel approach to laser ablation ICP-MS U-Pb geochronology data reduction, Geostandards and Geoanalytical Research, 36, 247–270, https://doi.org/10.1111/j.1751-908X.2012.00158.x, 2012.

Piccoli, P. M., and Candela, P. A.: Apatite in igneous systems, Reviews in Mineralogy and Geochemistry, 48, 255–292, https://doi.org/10.2138/rmg.2002.48.6, 2002.

Schaaf, P., Weber, B., Weis, P., Groβ, A., Ortega-Gutiérrez, F., and Kohler, H.: The Chiapas Massif (Mexico) revised: New geologic and isotopic data and basement characteristics, Neues Jahrbuch fur Geologie und Paläontologie, Abhandlungen, 225, 1–23, 2002.

Solari, L. A., Ortega-Gutiérrez, F., Elías-Herrera, M., Schaaf, P., Norman, M., Ortega-Obregón, C., and Chiquín, M.: U-Pb zircon geochronology of Palaeozoic units in western and central Guatemala: Insights into the tectonic evolution of Middle America, Geological Society, London, Special Publications, 328, 295–313, https://doi.org/10.1144/SP328.12, 2009.

Solari, L. A., Ortega-Gutiérrez, F., Elías-Herrera, M., Ortega-Obregón, C., Macías-Romo, C., Reyes-Salas, M.: Detrital provenance of the Grenvillian Oaxacan Complex, southern Mexico: a zircon perspective, International Journal of Earth Sciences, 103, 1301–1315, https://doi.org/10.1007/s00531-013-0938-9, 2014.

Spikings, R., Cochrane, R., Villagomez, D., Van der Lelij, R., Vallejo, C., Winkler, W., and Beate, B.: The geological history of northwestern South America: From Pangaea to the early collision of the Caribbean large igneous province (290–75 Ma), Gondwana Research, 27, 95–139, https://doi.org/10.1016/j.gr.2014.06.004, 2015.

Svojtka, M., and Košler: Fission-track dating of zircon by LA-ICP-MS, Goldschmidt Conference, Davos, Switzerland, Journal of Conference Abstracts, Special Supplement of Geochimica et Cosmochimica Acta, 66, A756, 2002.

Tera, F., and Wasserburg, G. J.: U-Th-Pb systematics in three Apollo 14 basalts and the problem of initial Pb in lunar rocks, Earth and Planetary Science Letters, 14, 281–304, https://doi.org/10.1016/0012-821X(72)90128-8, 1972.

Thomson, S. N., Gehrels, G. E., Ruiz, J., and Buchwaldt, R.: Routine low-damage apatite U-Pb dating using laser ablation–multicollector–ICPMS, Geochemistry, Geophysics, Geosystems, 13(2), https://doi.org/10.1029/2011GC003928, 2012.

Torres, R., Ruiz, J., Patchett, P. J., Grajales, J. M., Bartolini, C., Wilson, J. L., and Lawton, T. F.: Permo-Triassic continental arc in eastern Mexico: Tectonic implications for reconstruction of southern North America, , Geological Society of America, Special Papers, 340, 191–196, https://doi.org/10.1130/0-8137-2340-X.191, 1999.

Torres de León, R.: Caracterización geológica y geocronológica de unidades metamórficas e intrusivas de la región centro–Oeste de la Cuenca del Rio Motagua, Sureste de Guatemala, Centroamerica: implicaciones en las conexiones Sur de México–Bloque Chortís, Universidad Nacional Autónoma de México, Posgrado en Ciencias de la Tierra, Ph.D Thesis, 221 pp., 2016.

Vermeesch, P.: Statistics for LA-ICP-MS based fission track dating, Chemical Geology, 456, 19–27, https://doi.org/10.1016/j.chemgeo.2017.03.002, 2017.

Vermeesch, P.: IsoplotR: A free and open toolbox for geochronology, Geoscience Frontiers, 9, 1479–1493, https://doi.org/10.1016/j.gsf.2018.04.001, 2018.

Weber, B., Iriondo, A., Premo, W. R., Hecht, L., and Schaaf, P.: New insights into the history and origin of the southern Maya block, SE Mexico: U–Pb–SHRIMP zircon geochronology from metamorphic rocks of the Chiapas massif, International Journal of Earth Sciences, 96, 253–269, https://doi.org/10.1007/s00531-006-0093-7, 2007.

Weber, B., Valencia, V. A., Schaaf, P., Pompa-Mera, V., and Ruiz, J.: Significance of provenance ages from the Chiapas Massif Complex (southeastern Mexico): redefining the Paleozoic basement of the Maya Block and its evolution in a peri-Gondwanan realm, The Journal of Geology, 116, 619–639, https://doi.org/10.1086/591994, 2008.

Webster, J. D., and Piccoli, P. M.: Magmatic apatite: A powerful, yet deceptive, mineral, Elements, 11, 177–182, https://doi.org/10.2113/gselements.11.3.177, 2015.

Wolf, R. A., Farley, K. A., and Silver, L. T.: Helium diffusion and low-temperature thermochronometry of apatite, Geochimica et Cosmochimica Acta, 60, 4231–4240, https://doi.org/10.1016/S0016-7037(96)00192-5, 1996.

Zeitler, P. K., Herczeg, A. L., McDougall, I., and Honda, M.: U-Th-He dating of apatite: A potential thermochronometer, Geochimica et Cosmochimica Acta, 51, 2865–2868, https://doi.org/10.1016/0016-7037(87)90164-5, 1987.

Figure 1

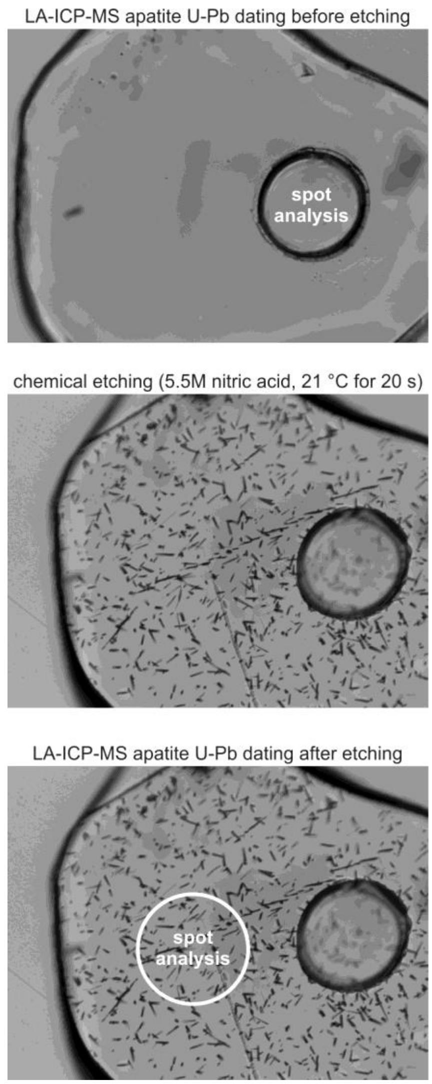
LA-ICP-MS apatite U-Pb dating before etching
spot analysis
chemical etching (5.5M nitric acid, 21 °C for 20 s)
LA-ICP-MS apatite U-Pb dating after etching
spot analysis

Figure 2

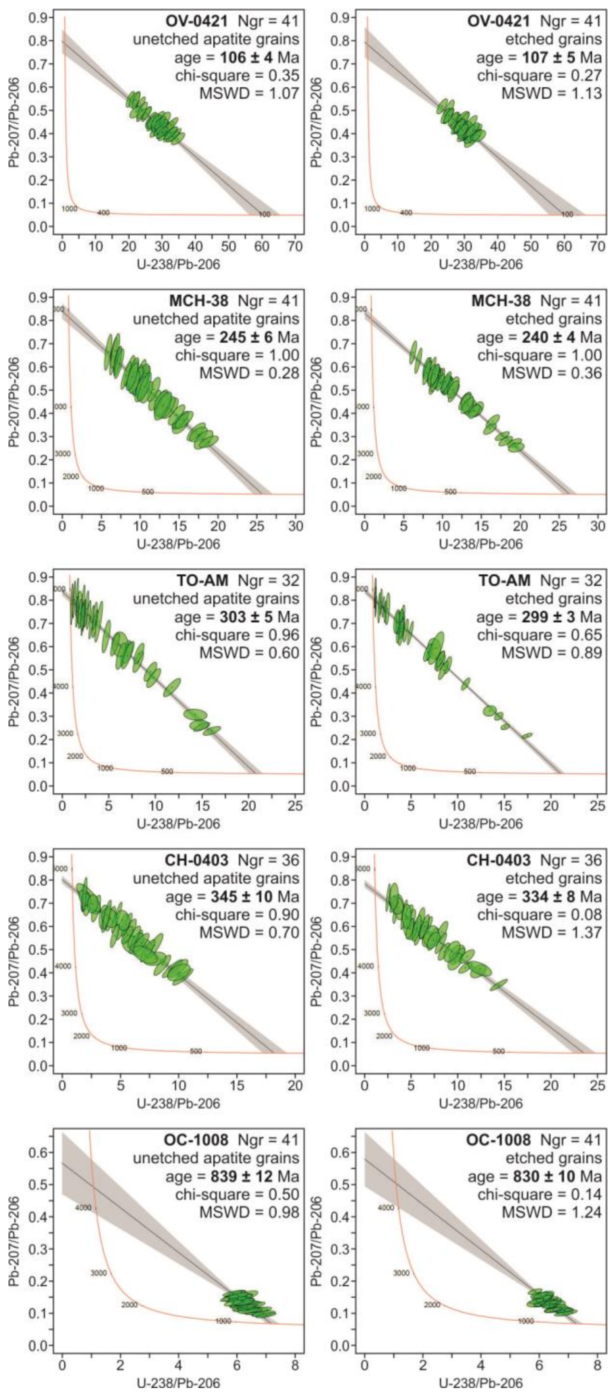
OV-0421 Ngr = 41
unetched apatite grains
age = 106 ± 4 Ma
chi-square = 0.35
MSWD = 1.07
OV-0421 Ngr = 41
etched grains
age = 107 ± 5 Ma
chi-square = 0.27
MSWD = 1.13
MCH-38 Ngr = 41
unetched apatite grains
age = 245 ± 6 Ma
chi-square = 1.00
MSWD = 0.28
MCH-38 Ngr = 41
etched grains
age = 240 ± 4 Ma
chi-square = 1.00
MSWD = 0.36
TO-AM Ngr = 32
unetched apatite grains
age = 303 ± 5 Ma
chi-square = 0.96
MSWD = 0.60
TO-AM Ngr = 32
etched grains
age = 299 ± 3 Ma
chi-square = 0.65
MSWD = 0.89
CH-0403 Ngr = 36
unetched apatite grains
age = 345 ± 10 Ma
chi-square = 0.90
MSWD = 0.70
CH-0403 Ngr = 36
etched grains
age = 334 ± 8 Ma
chi-square = 0.08
MSWD = 1.37
OC-1008 Ngr = 41
unetched apatite grains
age = 839 ± 12 Ma
chi-square = 0.50
MSWD = 0.98
OC-1008 Ngr = 41
etched grains
age = 830 ± 10 Ma
chi-square = 0.14
MSWD = 1.24
Pb-207/Pb-206
U-238/Pb-206

Figure 3

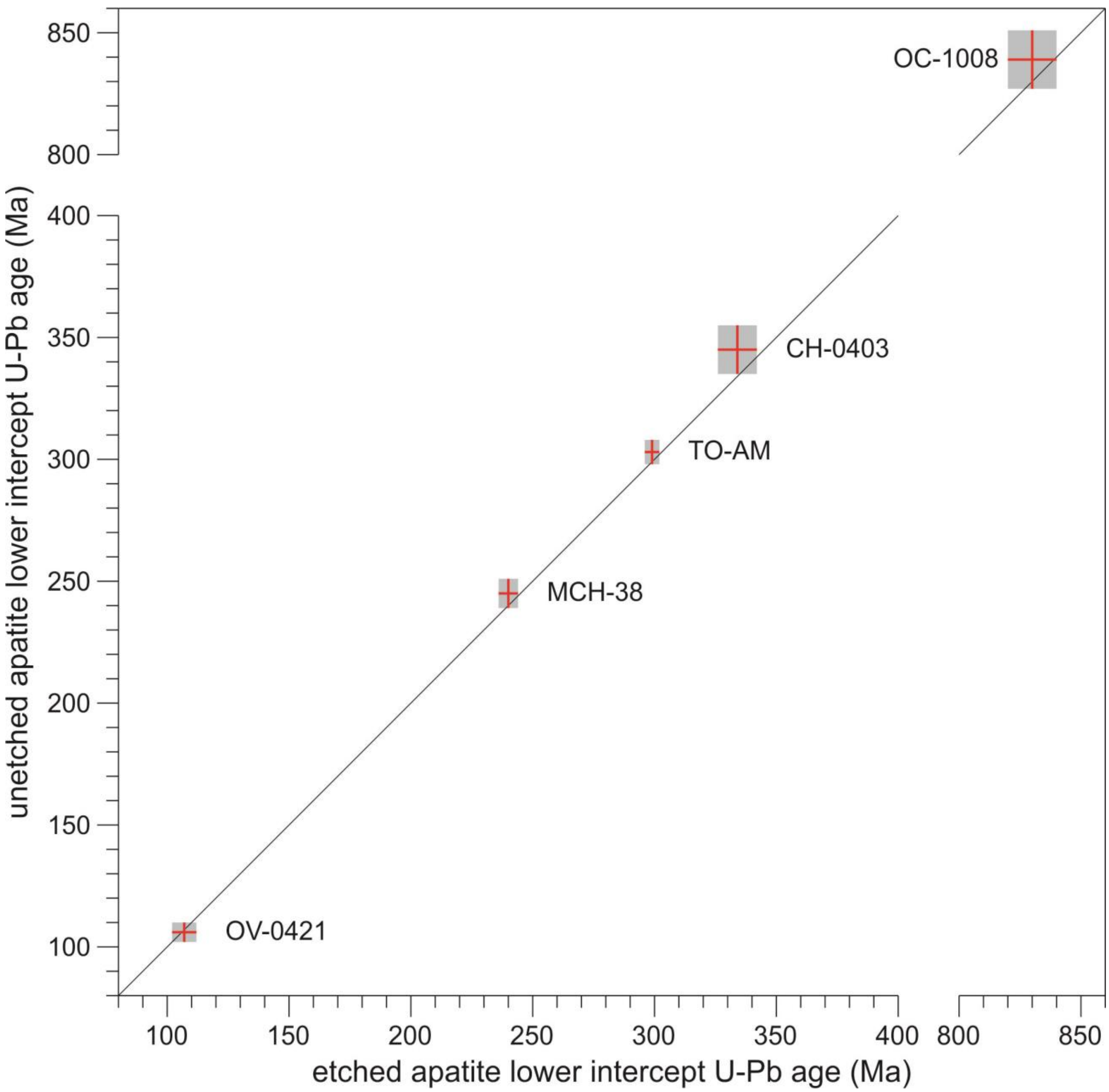
OC-1008
CH-0403
TO-AM
MCH-38
OV-0421
850
800
400
350
300
250
200
150
100
100
150
200
250
300
350
400
800
850
unetched apatite lower intercept U-Pb age (Ma)
etched apatite lower intercept U-Pb age (Ma)

Table 1

Lithology, locality, and zircon U–Pb data for the selected experimental rock samples.

Sample	Unit and locality	Rock type	Zircon U–Pb age	References
OV-0421	Tres Sabanas Pluton, Guatemala	deformed granite	115 ± 4 Ma	Torres de León (2016)
MCH-38	Chiapas Massif Complex, Mexico	orthogneiss	ca. 260 to ca. 252 Ma (?)	Weber et al. (2007, 2008)
TO-AM	Totoltepec Pluton, Mexico	granite	ca. 308 to ca. 285 Ma (?)	Kirsch et al. (2013)
CH-0403	Altos Cuchumatanes, Guatemala	granodiorite	391 ± 8 Ma	Solari et al. (2009)
OC-1008	Oaxacan Complex, Mexico	paragneiss	990 ± 10 Ma	Solari et al. (2014)

Table 2

LA–ICP-MS protocol established at LEI to be applied for simultaneous apatite U–Pb and fission-track in-situ double dating plus multielemental analysis (REEs, Y, Sr, Mn, Mg, Th, U, and Cl).

ICP-MS operating conditions	
Instrument	Thermo Scientific™ iCAP™ Qc
Forward power	1450 W
Carrier gas flow rate	~1 L/min (Ar) and ~0.35 L/min (He)
Auxiliary gas flow rate	~1 L/min
Plasma gas flow rate	~14 L/min
Nitrogen	~3.5 mL/min
Data acquisition parameters	
Mode of operating	STD (standard mode)
Sampling scheme	–2NIST-612–2MAD–1DUR–10apt–
Background scanning	15 s
Data acquisition time	35 s
Wash-out time	15 s
Measured isotopes	^{26}Mg ^{31}P ^{35}Cl ^{43}Ca ^{44}Ca ^{55}Mn ^{88}Sr ^{89}Y ^{139}La ^{140}Ce ^{141}Pr ^{146}Nd ^{147}Sm ^{153}Eu ^{157}Gd ^{159}Tb ^{163}Dy ^{165}Ho ^{166}Er ^{169}Tm ^{172}Yb ^{175}Lu ^{202}Hg ^{204}Pb ^{206}Pb ^{207}Pb ^{208}Pb ^{232}Th ^{238}U [total = 29]
Laser ablation system	
Ablation cell	RESOlution™ Laurin Technic *S-155*
Model of laser	Resonetics RESOlution™ *LPX Pro*
Wavelength	193 nm (Excimer ArF)
Repetition rate	4 Hz
Energy density	*4 J/cm^2
Mode of sampling	spot diameter of 60 µm

Note: MAD – "First mine Discovery" U–Pb apatite standard from Madagascar; DUR – Durango apatite from Cerro de Mercado mine (Mexico); apt – unknown apatite crystals. (*) Laser pulse energy of 4 J/cm^2, which was measured directly on target with a Coherent™ laser energy meter.